

Multi-stage heat treatment of aluminum alloy AA7049

R. RANGANATHA¹, V. ANIL KUMAR², VAISHAKI S. NANDI³, R. R. BHAT³, B. K. MURALIDHARA⁴

1. Mechanical Engineering, Sri Jagadguru Chandrasekarananthaswamiji Institute of Technology, Chikkaballapura, India;
2. Vikram Sarabhai Space Centre, Trivandrum, India;
3. Foundry & Forge Division, Hindustan Aeronautics Limited, Bangalore, India;
4. University Visvesvaraya College of Engineering, Bangalore, India

Received 27 July 2012; accepted 19 December 2012

Abstract: High strength 7xxx series aluminum alloys in the T6 temper are known to be highly susceptible to stress corrosion cracking (SCC). Retrogression and re-aging (RRA) is a heat treatment by which the resistance to SCC is enhanced without losing yield or tensile strength. The influence of multi-stage heat treatment on the properties and microstructure of AA7049 aluminum alloy was investigated. The microstructure of the alloy in various temper conditions was correlated to the electrical conductivity measurements, DSC analysis and TEM observation. The DSC analysis shows that RRA treatments lead to significant change in the microstructure and the resultant RRA precipitate microstructure is significantly different from both the T6 and T73 microstructures and is able to retain the strength of T6 temper while attaining the thermodynamic stability of the T73 temper.

Key words: aluminum alloy AA7049; retrogression; re-aging; heat treatment

1 Introduction

High strength aluminum alloys are used extensively in aerospace industry. Besides 2xxx series, 7xxx series Al–Zn–Mg–Cu alloys have been emerging as competitive and attractive candidate material for such applications primarily because of their higher specific strength. These alloys are known to be susceptible to corrosion in the peak strength state (T6 temper condition). The susceptibility of T6 temper to corrosion is alleviated through the use of over-aged T73 temper, which provides improved corrosion resistance, but with a 10%–15% reduction in strength [1].

In 7xxx aluminum alloys, the sequence of precipitation from supersaturated solid solution (SSS), metastable η' causes the peak hardening. GP-I and/or GP-II zones are considered to be precursors to the η' phase. The two types of GP zones have different structures and are formed on different preferential planes of the Al matrix and at different temperatures of quenching and aging. The GP zone and η' phase are formed in the early stage of precipitation. The control of size and volume fraction of these phases during the early

stages is important for obtaining optimized properties in the 7xxx aluminium alloys [2]. The morphology, chemical composition, size and shape of η' phase have been widely studied. The η' and η phases have been found to be of the composition that can be closely approximated to $MgZn_2$. These phases have hexagonal plate-like structure that grow preferentially on the {111} plane of the Al matrix [2–4].

Experimental results by CINA and GAN [5] indicated that retrogression and re-aging (RRA), a multi-stage heat treatment, is a trade-off between strength in T6 temper and corrosion resistance in T73 temper. The RRA consists of double aging treatment, with an intermediate retrogression (partial annealing) step. The first aging corresponds to the T6 temper, and the retrogression consists of partial annealing at temperature usually between 180 °C and 240 °C for a short time ranging from 2 min to 60 min, followed by water quenching. Finally, the alloy is re-aged at conditions similar to T6 temper.

Studies have also been conducted to characterize the microstructural differences under various heat treatment conditions, in order to gain insight into which microstructural parameters control the corrosion

susceptibility of this alloy. It is observed that the microstructure of AA7075-T73 shows grain boundary precipitates that are much coarser than those in the T6 temper. Furthermore, it has been shown that longer retrogression time during the RRA treatment leads to a combination of grain boundary precipitate coarsening, which resembles the precipitates formed in the T73 temper and the precipitate distribution in the matrix resembles the precipitates formed in the T6 temper. This combination results in good performance with respect to both resistance to stress corrosion cracking and mechanical strength [6–9].

The purpose of this study is to investigate the effect of RRA on the mechanical properties and the evolution of microstructure of AA7049 high strength aluminum alloy. The published information on the effect of various temper conditions such as T6, RRA for this alloy is very limited. In the present work, an attempt is made to examine the tensile properties and correlate the phase transformations that occur during RRA using differential scanning calorimetry (DSC) and transmission electron microscopy (TEM) with electrical conductivity measurements.

2 Experimental

The raw material AA7049 alloy for this study was in the form of extrusion of 65 mm diameter and 160 mm length with a chemical composition listed in Table 1.

Table 1 Specified and obtained chemical composition of AA7049 alloy

Element	Composition/%	
	Specified	Actual
Zn	7.2–8.4	7.82
Mg	2.1–3.1	2.23
Cu	1.2–1.9	1.44
Fe	≤0.5	0.22
Si	≤0.4	0.25
Mn	≤0.5	0.29
Ti and Zr	≤0.5	0.16
Al	Bal.	Bal.

The extrusions were checked for soundness using ultrasonic flaw detector (Kraut Kramer make) with 2 mm flat bottom hole (FBH) standard reference block. The acceptance standard used was Class A as per AMS 2630B. The extruded rods were ascertained for absence of defects like cracks, porosity or cavity. The properties of the extruded raw material were evaluated on six samples and the results are given in Table 2.

In the present work, heat treatment was carried out to three different tempers, viz, T6, T73 and T77. All the

Table 2 Properties of as-received AA7049 extruded rods

Hardness (BHN)	Conductivity/ % IACS	$\sigma_{0.2}$ / MPa	UTS/ MPa	Elongation/ %
85–89	37.9–38.8	226–230	311–313	12.07–12.93

samples were solution treated at 470 °C with a soaking duration of 120 min and then water quenched. These samples were aged to different tempers. The maximum time delay between quenching and aging was 15 min. For attaining T6 temper, the solution treated samples were aged at 120 °C for 24 h. Similarly, for attaining T73 temper the solution treated samples were left for natural aging for a period of 48 h. These samples were then subjected to two steps of artificial aging of 120 °C for 24 h, air cooling to room temperature followed by aging at 160 °C for 14 h and air cooling to room temperature. For RRA treatment all specimens were initially heat treated to T6 temper and then subjected to RRA heat treatment (T77) which consisted of retrogression treatment at 180–240 °C, for a duration varying from 2 min to 60 min. All the specimens were water quenched after retrogression and subsequently re-aged at 120 °C for 24 h. After aging treatment the samples were air-cooled to room temperature.

All the heat treated samples were evaluated for mechanical properties using TIRA universal testing machine at room temperature in accordance with ASTM E-8M standard. A Max Electronics conductivity meter, having range of 10% to 120% IACS (International Annealed Copper Standard) where 1%IACS=0.58 MS/m, was used to perform electrical conductivity measurements of the heat treated samples. Universal V4 2E TA Instruments DSC Q100 thermal analysis processing unit was used for carrying out differential scanning calorimetry experiments. The tests were run in nitrogen atmosphere with a heating rate of 20 °C/min, and in the temperature range of 25 °C to 500 °C. Disc-shaped heat treated samples of 30 mg mass enclosed in aluminum capsules were tested. The microstructure was characterized using a Philips CM20 TEM operating at 200 kV.

3 Results and discussion

The variations in UTS and $\sigma_{0.2}$ with different heat treatment tempers, i.e T6, T73 and RRA in longitudinal direction are plotted in Figs. 1 and 2, respectively. The UTS for T6 temper was 660 MPa and was 564 MPa for T73 temper. Similarly, the conductivity for T6 temper was 30.4%IACS and 35%IACS for T73 temper as shown in Fig. 3. From Figs. 1 and 2, it is evident that at lower retrogression temperature of 180 °C, the UTS value achieved is marginally higher than or in line with that of T6 temper irrespective of retrogression durations

employed in this investigation. At higher temperature of 200 °C to 240 °C, it is seen that UTS is maintained at T6 temper level up to 10 min of retrogression time and there is appreciable drop in UTS at higher retrogression durations beyond 10 min.

The $\sigma_{0.2}$ is superior to T6 temper for all retrogression treatments at temperature of 180 °C and time durations up to 20 min in the remaining temperatures 200 °C to 240 °C. This is further supported by the fact that at lower retrogression temperature of 180–200 °C there is appreciable increase in conductivity in the range of 32%–36% IACS when compared with the conductivity of 30% IACS in T6 temper. At higher retrogression temperature and time duration beyond 30 min, there is steep increase in electrical conductivity up to 40% IACS. The corresponding drop in strength is also steeper in case of higher retrogression time and temperature as compared to lower temperature and time regime. From Figs. 1, 2 and 3, it is clear that the electrical conductivity has an exactly reverse trend to strength.

The variation in physical and mechanical properties of the aluminum alloys is attributed to the various precipitation stages formed during the multi stage heat

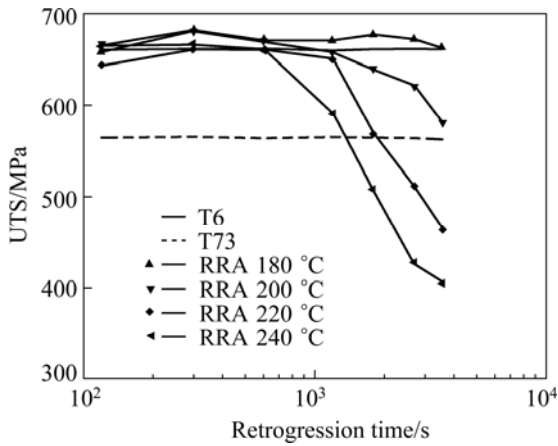


Fig. 1 Variation of tensile strength with retrogression time

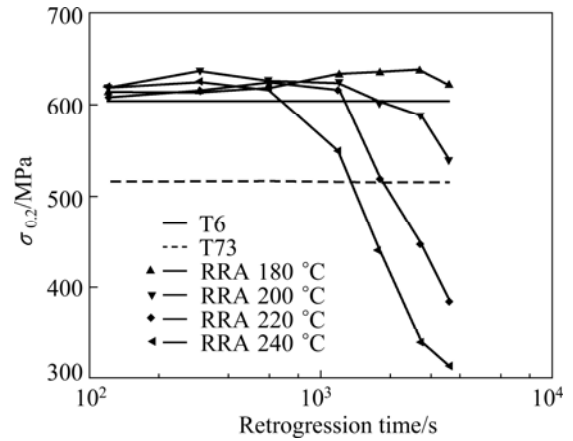


Fig. 2 Variation of $\sigma_{0.2}$ with retrogression time

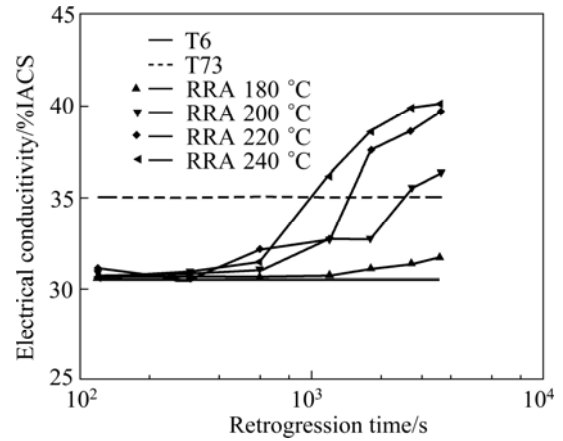


Fig. 3 Variation of electrical conductivity with retrogression time

treatment. In general, for high strength aluminum alloys (7xxx series) the precipitation sequence from the supersaturated solid solution (SSS) may be represented as $SSS \rightarrow GP \text{ zones} \rightarrow \eta'(\text{semi-coherent } MgZn_2) \rightarrow \eta(\text{incoherent } MgZn_2)$ [9,10].

TEM micrograph of the alloy in peak aged T6 temper condition revealed a very fine precipitate of GP

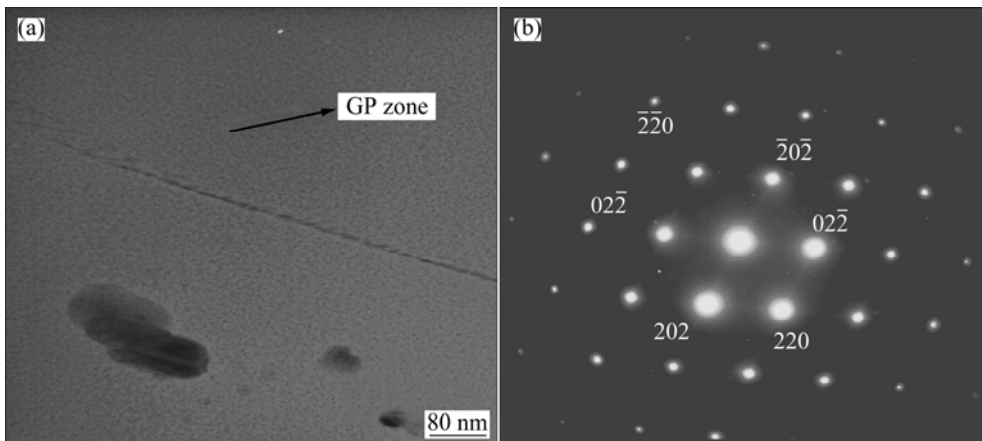


Fig. 4 Bright field TEM image of alloy in T6 temper (a) and SAED pattern near $[110]_{Al}$ corresponding to Fig. 4(a) (b)

zones distributed homogeneously inside the grains with coarser and less spaced η' grain boundary precipitates, as can be seen in Fig. 4(a). The presence of fine precipitate structure of GP zones and metastable phase η' are attributable to the strengthening of alloy. The selected area electron diffraction (SAED) analysis in this study indicated that the majority of the precipitates are of η' type and more stable GP-II zones are present in smaller amount as seen in Fig. 4(b). TEM micrograph of the

alloy in over-aged T73 temper condition (Fig. 5(a)) shows coarser precipitates with uniform distribution inside the grains. The SAED pattern for the alloy in T73 temper (Fig. 5(b)) reveals several spots from the equilibrium precipitate η and less from η' . These precipitates are essentially η with η' precipitates present in a smaller extent. The microstructures resulting from RRA temper (Fig. 6(a) and Fig. 7(a)) are similar to that of T6 temper in the sense that there is a fine distribution

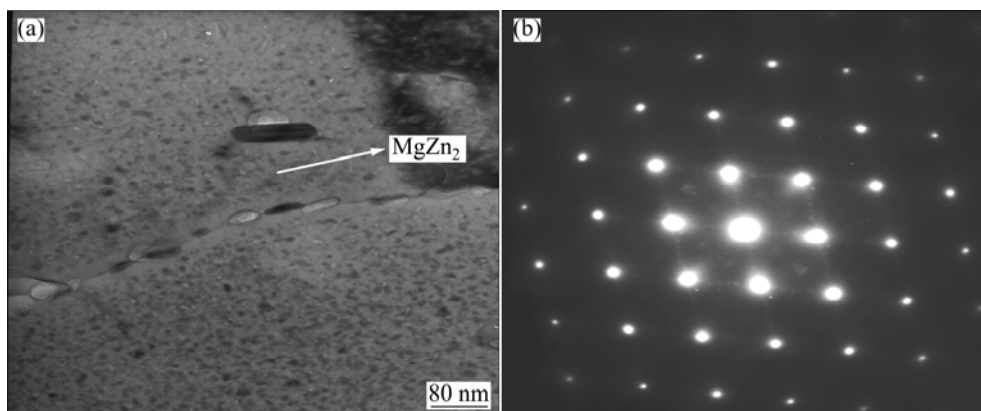


Fig. 5 Bright field TEM image of alloy in overaged T73 temper (a) and SAED pattern near $[110]_{Al1}$ corresponding to Fig. 5(a) (b)

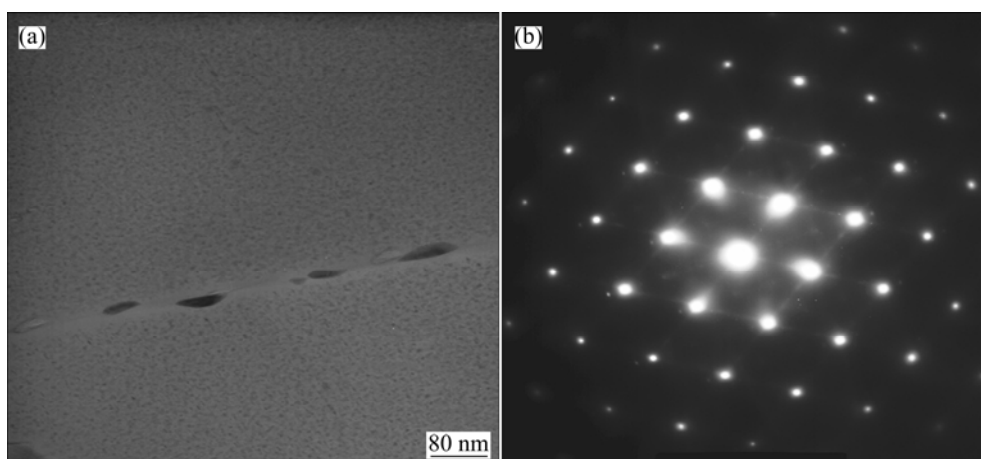


Fig. 6 Bright field TEM image of alloy after RRA at 180 °C for 10 min (a) and SAED pattern near $[110]_{Al1}$ corresponding to Fig. 6(a) (b)

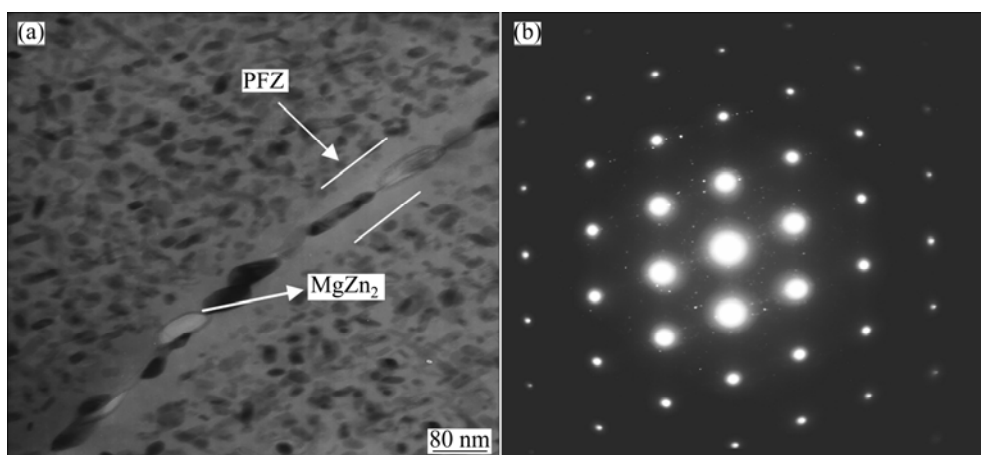


Fig. 7 Bright field TEM image of alloy after RRA at 240 °C for 60 min (a) and SAED pattern near $[110]_{Al1}$ corresponding to Fig. 7(a) (b)

of η' precipitates in the aluminum matrix grains, and the coarser η precipitates which are distributed in the matrix are similar but bigger in size compared to that in T73 temper (Fig. 5(a)). The observations are in close agreement with those in the literatures [11,12].

The precipitate morphology observed under transmission electron microscope (TEM) is further supported by the DSC thermograms shown in Fig. 8. The curve for T6 temper has three peaks: endothermic peak I (dissolution reaction) at low temperature, doublet exothermic peak IIa and IIb (precipitation reaction) at intermediate temperature and endothermic peak III at a further higher temperature. The calorimetric results of the T6 temper samples in this work are in close agreement with those in the literatures [9–11,13,14]. The first endothermic reaction is a result of the dissolution of GP zones. As the temperature increases, the dissolution of the coarser and more stable η' phase overlaps the η phase precipitation occurring during the lower temperature exothermic peak IIa (225.9 °C); whilst the exothermic peak IIb (249.6 °C) is a result of coarsening of η phase by an Ostwald ripening process [15]. The curve in T73 temper shows two endothermic regions. The low temperature region has a peak temperature which is higher than the low temperature region of T6 curve (Table 3). The calorimetric curve in T73 temper shows the low temperature endothermic peak resulting principally from the dissolution of preexisting η' . Some η formation and growth also take place, but this is to a lesser extent. The second endothermic peak is due to the dissolution of η' phase.

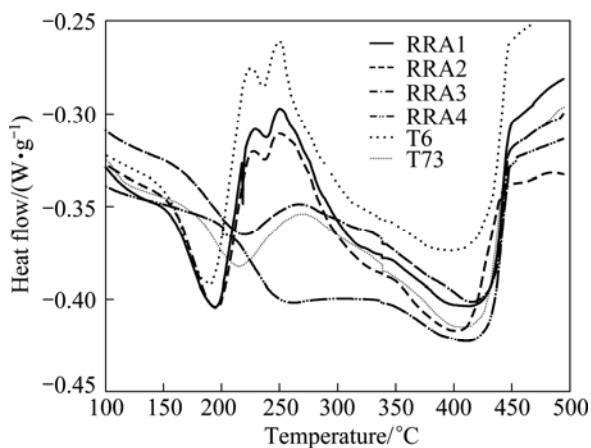


Fig. 8 DSC thermograms of AA 7049 alloy in various tempers

The materials in various RRA conditions show a transitional type behavior in the DSC [9,13]. It is seen from Fig. 8 that RRA causes a pronounced change in the shape of the thermogram as evident from the changes in the microstructure. The changes in the characteristics of DSC curves from T6 to RRA4 conditions occur in peaks I and II regions of the curves. The peak I temperature

Table 3 Exothermic and endothermic peak temperatures for different tempers derived from DSC thermograms

Temper	Peak temperature/°C			
	I	IIa	IIb	III
T6	194.8	225.9	249.6	429
RRA1 (180 °C, 30 min)	198.6	229.6	250.9	434
RRA2 (200 °C, 5 min)	199.6	224.6	249.1	432
RRA3 (220 °C, 45 min)	223.8	–	–	435
RRA4 (240 °C, 60 min)	243.6	–	–	432
T73	209.1	–	–	430

increases from 194.8 °C (T6) to 243.6 °C (RRA4) and the region becomes more diffuse and broad with increased retrogression temperature and time. RRA has a similar influence on the peak II region. The doublet formed in T6 is suppressed gradually by the retrogression. Also peak II vanishes with increase in RRA temperature and time. This is because the expected exothermic contribution is over-riding the endothermic contribution of the η' precipitates that dissolve on heating the sample during DSC run. This indicates that the RRA microstructure has higher volume fraction of η precipitate. Finally, η dissolution is revealed by high temperature endothermic peak. The RRA heat treatment cleans up aluminum matrix by forming more thermodynamically stable η precipitates thereby reducing the matrix supersaturation, and hence the electrical conductivity increases compared to that in T6 temper. RRA with longer time and higher temperature causes rapid over-aging and large coarsening of precipitate, which results in reduction in strength. The electrical conductivity of 40%IACS at RRA4 reveals that the material is over-aged, and the corresponding DSC curve for RRA4 condition indicates that there is no precipitation formation in that condition and only the dissolution of coarser precipitate occurs.

4 Conclusions

1) The T6 temper microstructure consists of a high density of fine precipitates distributed homogeneously in the aluminum matrix; the precipitates are essentially η' and small amounts of fine GP zones and η are also coexistent.

2) During retrogression, the dissolution of less stable precipitates (GP zones and the finer particles of η') inside the grains happens. The amount of dissolution is controlled by the retrogression temperature. Temperatures above 180 °C are more efficient in dissolving the precipitates. Also the grain boundary precipitates grow and become more spaced.

3) During re-aging, re-precipitation of η' happens and at the same time the pre-existent particles grow and transform to stable η . The microstructure inside the grains is similar to that in T6 temper, but the precipitates are slightly denser and coarser. The volume fraction of η rises during the RRA treatment. The resulting final grain boundary microstructure is similar to that in overaged T73 temper.

4) The greater the retrogression temperature is, the more stable the microstructures are after re-aging. Thus the retrogression temperature influences the microstructural stability after re-aging.

5) In the microstructure of samples subjected to RRA treatment, i.e. reaging treatment after retrogression step, the precipitates η' and η are dispersed in the alloy matrix along with coexistent coarser and sparsely distributed η precipitates which decorate the grain boundaries, together with precipitate free zones (PFZs). This makes it possible to retain the strength of T6 temper while attain the thermodynamic stability of the T73 temper.

Acknowledgments

The authors thank Dr. K. Satya Prasad, Scientist F, and Dr. M. Vijaykumar, Scientist G, DMRL, Hyderabad for extending support in carrying out this research work. The authors are also thankful to Directors, VSSC & HAL for granting permission to publish this work.

References

- [1] FERRER C P, KOUL M G, CONNOLLY B J. Low temperature retrogression and re-aging heat treatments for thick section components of aluminum alloy 7075 for aging aircraft refurbishment [C]//MANTZ R A, TRULOVE P C. Tri-Service Corrosion Conference. 2002. AMTIAC Document No: AM025816.
- [2] SHA G, CERZO A. Early-stage precipitation in Al–Zn–Mg–Cu

- alloy (7050) [J]. Acta Mater, 2004, 52: 4503–4516.
- [3] SHA G, CERZO A. Characterization of precipitates in an aged 7xxx series Al alloy [J]. Surf Interface Anal, 2004, 36: 564–568.
- [4] BIGOT A, DANOIX F, AUGER P, BLAVETTE D, REEVES A. Tomographic atom probe study of age hardening precipitation in industrial AlZnMgCu (7050) alloy [J]. Mater Sci For, 1996, 217–222: 695–700.
- [5] CINA B M, GAN R. Reducing the susceptibility of alloys particularly aluminum alloys to stress corrosion cracking. US Patent 3856584 [P]. 1974: 12–24.
- [6] DANH H C, KRISHNA RAJAN, WALLACE W. A TEM study of microstructural changes during RRA in 7075 aluminium alloy [J]. Metall Trans A, 1983, 14: 1843–1850.
- [7] PARK J K, ARDELL A J. Effect of retrogression and re-aging treatments on the microstructure of Al-7075-T651 [J]. Metall Trans A, 1984, 15: 1531–1543.
- [8] RAJAN K, WALLACE W, BEDDOES J. Microstructural study of the high strength stress corrosion resistant 7055 aluminium alloy [J]. Mater Sci, 1982, 17: 2817–2824.
- [9] VIANA F, PINTO A M P, SANTOS H M C, LOPES A B. Retrogression and re-ageing of 7075 aluminium alloy: Microstructural characterization [J]. Mater Proc Tech, 1999, 92–93: 54–59.
- [10] LOFFLER H, KOVACS I, LENDVAI J. Review: Decomposition processes in Al–Zn–Mg alloys [J]. Mater Sci, 1983, 18: 2215–2240.
- [11] BALDANTONI A. On microstructural changes during the retrogression and re-aging of 7075 type aluminium alloy [J]. Mater Sci Eng, 1985, 72: L5–L8.
- [12] GAZDA A, WARMUZEK M, WIERZCHOWSKI W. DTA investigation of the retrogression and re-aging in some Al–Zn–Mg–Cu alloys [J]. Thermochem Acta, 1997, 303: 197–202.
- [13] OLIVEIRA A F, de BARROS M C, CARDOSO K R, TRAVESSA D N. The effect of RRA on the strength and SCC resistance on AA 7050 and AA 7150 aluminium alloys [J]. Mater Sci Eng A, 2004, 379: 321–326.
- [14] PAPAIZIAN J M. Differential scanning calorimetry evaluation of retrogressed and re-aged microstructures in aluminium alloy 7075 [J]. Mater Sci Eng, 1986, 79: 97–104.
- [15] PARK J K, ARDELL A J. Correlation between microstructure and calorimetric behavior of aluminium alloy 7075 and Al–Zn–Mg alloys in various tempers [J]. Mater Sci Eng A, 1989, 114: 197–203.

多级热处理工艺对铝合金 AA7049 性能的影响

R. RANGANATHA¹, V. ANIL KUMAR², VAISHAKI S. NANDI³, R. R. BHAT³, B. K. MURALIDHARA⁴

1. Mechanical Engineering, Sri Jagadguru Chandrasekarananthaswamiji Institute of Technology,

Chikkaballapura, India;

2. Vikram Sarabhai Space Centre, Trivandrum, India;

3. Foundry & Forge Division, Hindustan Aeronautics Limited, Bangalore, India;

4. University Visvesvaraya College of Engineering, Bangalore, India

摘要: T6 态高强 7xxx 系列铝合金对应力腐蚀开裂敏感。采用回归和再时效热处理(RRA)可以提高其抗应力腐蚀开裂性能而不降低其强度性能。研究了多级热处理工艺对 7049 铝合金性能和组织的影响。通过电导率测量、DSC 分析和 TEM 组织观察, 考察合金在不同热处理态的组织变化。DSC 分析表明, RRA 处理会导致合金的显微组织发生显著变化, RRA 处理态合金的组织与 T6 和 T73 态合金的组织明显不同。RRA 处理可以使合金保持在 T6 态的强度且获得 T73 态的热力学稳定性能。

关键词: 铝合金 AA7049; 回归处理; 再时效; 热处理